



Contents lists available at ScienceDirect

Arabian Journal of Chemistry

journal homepage: www.ksu.edu.sa

Original article

Hansen parameters and GastroPlus assisted optimized topical elastic liposomes to treat breast cancer using a novel isatin derivative



Mohammad A. Altamimi^a, Afzal Hussain^{a,*}, Mohammed M. Alanazi^b, Dhafer Alotaibi^a, Saeed Ali Syed^c, Ahmed Bari^c

^a Department of Pharmaceutics, College of Pharmacy, King Saud University, Riyadh 11451, Saudi Arabia

^b Department of Pharmacology and Toxicology, College of Pharmacy, King Saud University, Riyadh, Saudi Arabia

^c Department of Pharmaceutical Chemistry, College of Pharmacy, King Saud University, Riyadh 11451, Saudi Arabia

ARTICLE INFO

Keywords:

TM-19
HSPiP and QbD
GastroPlus
Topical elastic liposomes
MCF-7

ABSTRACT

Breast cancer treatment is a global health challenge using conventional toxic chemotherapeutic agents. A novel isatin could be a promising alternative. An isatin derivative (TM-19) was synthesized and characterized using NMR (nuclear magnetic resonance), mass spectrometry, Fourier transform infrared (FTIR), and differential scanning calorimetry (DSC). HSPiP and GastroPlus predictive software were used to predict suitable solvents for solubility and in vivo oral pharmacokinetics in humans (fasted condition), respectively. Based on predictive findings, topical elastic liposomes (phosphatidylcholine as PC and span 80 by film hydration method) was prepared, characterized, and optimized using QbD (quality by design). QbD identified the impact of composition on response variables (Y₁ for size, Y₂ for polydispersity index, Y₃ for zeta potential, and Y₄ for %EE). In vitro cytotoxicity study was carried out against MCF-7 cell lines. Low molecular weight and lipophilic TM-19 was crystalline in nature (255 g/mol). GastroPlus program predicted limited in vivo dissolution and poor oral absorption (10.4 %). Results confirmed the highest TM-19 solubility in DMSO (dimethyl sulfoxide) > chloroform > PEG 400 (polyethylene glycol 400). Considering experimental and predicted data, topical delivery of TM-19 using optimized (desirability parameter value = 0.97) elastic liposomes (TF1) was quite promising due to optimal size (344 nm), high %EE (61.7 %), low PDI (0.45), and optimal zeta potential (− 12.34 mV). TM-19 loaded TF1 elicited concentration dependent cytotoxic effect (> 90 % at 10 μM) against MCF-7 as compared to TM-19 suspension.

1. Introduction

Breast cancer is a major cause of mortality among women worldwide, with 2.3 million cases and 685,000 deaths reported in 2020 (World Health Organization, 2022). While chemotherapy is the first line of treatment, issues such as disease progression, metastasis, delayed detection, and multi-drug resistance remain a challenge for healthcare professionals and scientists. Additionally, drug related toxicity, and severe side effects, reduce patient compliance, highlighting the need for an alternative compound with potential efficacy with reduced adverse effects.

In this study, imine compounds have been synthesized for various therapeutic applications, including anticancer properties. Thiophene-3-carboxaldehyde was selected in the present study based on its established biological activity in various literatures, including its use as an

intermediate in the synthesis of various biologically distinct molecules (Altamimi et al., 2020; Bergman et al., 1988; McKerrowb et al., 2003; Saliva et al., 2001). 1H-indole-2,3-dione (isatin) is a heterocyclic natural product found in plants of the genus *Isatis* and is also present in humans as a metabolic derivative of adrenaline (Bergman et al., 1988; Saliva et al., 2001). Its pharmacological properties, such as antimicrobial, anticancer and anti-proliferative effects, have made it increasingly important in the field of drug discovery (McKerrowb et al., 2003; Guo and Diao, 2020). Moreover, chemical modifications have shown to improve the safety profiles of various drugs, allowing for synthetic modifications that result in more potent analogues with reduced toxicity.

Newly synthesized compound, which make up about 40 % of new chemical entities, often faces challenges related to physicochemical properties that are unsuitable for successful drug delivery and achieving

* Corresponding author at: Department of Pharmaceutics, College of Pharmacy, King Saud University, Riyadh 11451, Saudi Arabia.

E-mail addresses: afzal.pharma@gmail.com, amohammed2@ksu.edu.sa (A. Hussain).

<https://doi.org/10.1016/j.arabjc.2024.106028>

Received 15 April 2024; Accepted 15 October 2024

Available online 18 October 2024

1878-5352/© 2024 The Author(s). Published by Elsevier B.V. on behalf of King Saud University. This is an open access article under the CC BY-NC-ND license (<http://creativecommons.org/licenses/by-nc-nd/4.0/>).

desired outcomes (Bhalani et al., 2022). These challenges include poor aqueous solubility, limited in vitro-in vivo dissolution, low in vivo absorption, and subsequently poor oral bioavailability. However, formulation scientists can modify such physicochemical properties of the newly synthesized compound to make them suitable for formulation development and drug delivery. These approaches include prodrug synthesis, conjugation, salt formation, nanonization, complexation, nanocarriers as drug delivery, and surfactant-solvent mediated improved solubility.

developing a new compound and successful transitioning it to clinical use is a long journey for scientists. Therefore, various software program-based prediction and simulation approaches reduced substantial preliminary assessment duration in drug discovery and formulation development. HSPiP software is well explored in paint industry, drug delivery, and confectionary products. HSPiP is based on the total cohesive energy of material primarily distributed over dispersion energy, polarity energy, and hydrogen bonding formation energy. These three energies are expressed as Hansen solubility parameters (HSP) of HSPiP, where, δ_d , δ_p , and δ_h represent dispersion parameters, polarity parameter and hydrogen bond parameter, respectively. HSPiP classified solvents as “bad” or “good” based on the estimated RED (relative energy difference) value. A solvent with RED value < 1 was considered as a “good” solvent to solubilize the modeled solute in HSPiP and vice versa (Hansen, 2007; Abbott, 2012). Similarly, GastroPlus is a predictive and simulative program for pharmacokinetic and pharmacodynamics prediction and simulation in various animal models and human with fast or fed condition. This is widely used in pharmaceutical and academic level for generic products based on experimental and literature-based data. The GastroPlus is approved by US FDA to waive in vivo clinical study for a generic product with available data. GastroPlus predicts, in vivo dissolution, in vivo absorption, in vivo regional absorption, and the impact of various critical attributes on pharmacokinetic parameters. Recently, we explored various studies to predict and simulate in vitro dissolution performance of poorly soluble drugs in human using GastroPlus (Hussain et al., 2022a; Aljurbui et al., 2022; Hussain et al., 2020a). Oral delivery is the most preferred route of administration over others. However, several challenging issues are associated for oral delivery of anticancer drugs in order to treat breast cancer. GastroPlus predicted limited oral in vivo absorption in humans. The predicted data was used to rationalize topical delivery of TM-19.

In this study, we synthesized TM-19, a new isatin derivative, and evaluated its cytotoxic potential against MCF-7. Furthermore, NMR (nuclear magnetic resonance), FTIR (Fourier Transform Infrared), and DSC (differential scanning calorimeter) for their respective positions corresponding to aromatic and NH groups, and thermal behavior, respectively, were used for evaluations. Mass spectra also confirms the presence of molecular ion peak confirming the proposed molecule. On the other hand, based on the predicted results using HSPiP and GastroPlus, transdermal drug delivery was preferred as the route of administration over oral and parenteral dosage form due to several advantages and improved patient compliance. Several attempts have been made to improve TM-19's poor solubility and absorption by tailoring it as vesicular or nanocarrier systems to control breast cancer delivery through follicular and non-follicular routes of permeation across stratum corneum of skin [11–12] (Kyounghee et al., 2018; Altamimi et al., 2021a).

TM-19 was solubilized in various solvents, oil, and surfactants. Before being formulated in elastic liposomes with varying phospholipid (phosphatidylcholine) and span 80 contents. Several trial formulations were prepared and characterized for parameters such as vesicle size, PDI, zeta potential and entrapped drug, using experimental design tool as pre-optimization step. A mixed design model suggested various compositions considering two factors (PC as X_1 and span 80 as X_2) at two levels and four responses (size as Y_1 , PDI as Y_2 , zeta potential as Y_3 , and %entrapment efficiency as Y_4). The robust formulation was selected based on the desirability numerical parameter under given constraints

and importance. The optimized formulation, TF1, was prepared and evaluated for various parameters and compared with TM-19 suspension (Altamimi et al., 2021b). Finally, the optimized formulation was evaluated for anticancer potential against MCF-7 at varied concentrations and compared to pure drug suspension.

2. Materials and methods

2.1. Materials

TM-19 was synthesized in our laboratory. Ethanol, span 80, PC and acetonitrile were procured from Sigma Aldrich, (USA). Buffer reagents were obtained from Sigma Aldrich, United States of America. Phosphatidylcholine was procured from Merck, USA. Chloroform (analytical grade) was procured from Fisher Scientific, Bishop Meadow Road, Loughborough, UK. These reagents were of analytical grade. Milli-Q water was used as an aqueous solvent. HSPiP and GastroPlus were procured for simulation and prediction (USA).

3. Methods

3.1. Synthesis of isatin hydrazone and TM-19

TM-19 was synthesized following a reported method with slight modifications (Singh et al., 2020). Isatin (1 mmol) was added in ethanol followed by hydrazine hydrate (1.1 mmol) in a round bottom flask. A few drops of acetic acid were added as a catalyst and the reaction mixture was refluxed for 4 h with stirring. Ice was added and the precipitate obtained was washed several times with water. Using the intermediate product, equimolar quantities (1.1 mmol) in ethanol, was add 3-thiophencarboxyaldheyed followed by few drops of acetic acid the mixture was refluxed for 3 h. After completion of reaction ice was add and the precipitate obtained (TM-19) was filtered and washed with water.

3.2. TM-19 identification using various spectroscopic methods

The obtained solid material of TM-19 was characterized by spectroscopic methods (NMR and MS). The ^1H - and ^{13}C NMR spectra were recorded on a Bruker instrument at 500 and 700 MHz for ^1H and 176 MHz for ^{13}C at 295 K in $\text{DMSO}-d_6$. The peaks were calibrated using TMS, which served as an internal standard in deuterated DMSO. Integration and peak picking were carried out using Bruker's standard method on topspin 3.1 software.

The mass spectrometric experiments were performed on a Jeol JMS-700 mass spectrometer using electron ionization (EI) technique at 70 eV to determine the molecular ion peak and other fragments. In the intermediate molecule spectra, molecular ion peak at 161 and a base peak at 104 confirmed the desired molecule. In the final product, a molecular ion peak at 255 along and a base peak at 227 confirmed the proposed molecule.

To assess the sample of TM-19 using ATR-FTIR, a (5 mg sample) was dissolved in ethanol and dropped onto the ATR crystal surface for drying. The dried sample was then subjected to FTIR assessment using ATR-FTIR (ATR-FTIR, Bruker Alpha, Germany). Each sample was scanned between 4000 and 400 cm^{-1} at 16 times to identify stretching and vibration related with functional groups of TM-19. TM-19 was accurately weighed and dissolved in acetonitrile to a final concentration of 0.1 mg/ml. This served as stock solution and was scanned using a UV Vis spectrophotometer (UV 1601PC, Shimadzu, Japan). Analytical grade acetonitrile was used as a blank to set the base line.

3.3. Analytical method

The analysis was performed using UPLC (ultra-performance liquid chromatography) system (Waters Acquity) equipped with PDA-detector.

Chromatographic separation was achieved using a reversed phase Acquity UPLC® BEH C18 (2.1 × 100 mm, 1.7 μm particle size) column. The chromatographic and integrated data were recorded using Empower 2 Software in the computed system. During the analytical method development of TM-19, a mobile phase with a variable proportion of water and acetonitrile was used for optimization and peak resolution. The mobile phase composition was further changed with a variable composition of 0.1 % formic acid and acetonitrile, followed by various proportion of 0.01 M KH₂PO₄ aqueous solution and acetonitrile. The mobile phase pH was optimized by running the sample at a varied pH range (2.5—6.0) followed by varied column temperatures. Finally, the optimized mobile phase composition contained 0.2 % formic acid (aqueous) and methanol (80 %) at pH = 6.0 and 40 °C (operating temperature). A 50 ppm solution of 3-((thiophen-3-ylmethylene) hydrazono) indolin-2-one (TM-19) was scanned over a range from 190.0 nm to 400.0 nm and the λ_{max} was observed at 341 nm.

Chromatographic separation was achieved on Acquity HPLC® BEH C₁₈ using a mobile phase consisting of mixture of pH 6.0 formic acid (0.2 % aqueous) and methanol (20:80 v/v) under isocratic mode of elution. The mobile phase was prepared, filtered using (0.2 μm) membrane filters, and sonicated (water bath sonicator) for 30 min to remove trapped air bubbles. Separation was performed using 0.2 mL/min flow rate at 40 °C, and the run time was 5 min. The injection volume was 2 μL and the detection wavelength was set at 341 nm. 100 ppm solution of TM-19 was prepared by dissolving the required amount of the compound in 80 % methanol. For accuracy, precision, linearity, limit of detection, and quantification tests, the solution were appropriately diluted with 80 % (aqueous) methanol.

3.4. HSPiP predicted solvents for TM-19 solubility

HSPiP was used to estimate HSP of TM-19 and various solvents. To accomplish this, various input parameters were loaded based on literature data, experimental data, and by-default settings. HSPiP estimated all HSP parameters such as δ_d, δ_p, δ_h, δ, MVol, density, fusion enthalpy, and H-donor and acceptor count ratio. The selection of solvent was based on the minimum difference of each HSP value between TM-19 and solvent using HSPiP. HSP values were determined for each solvent and were compared with the TM-19. The closeness of each HSP value between TM-19 and solvent/surfactant/co-surfactant indicate the degree of solubility/miscibility as estimated in HSPiP (Singh et al., 2021). Furthermore, the experimental solubility was carried out in the selected solvents (as predicted in HSPiP) to find quantitative values. Moreover, HSPiP used to predict and simulate in vitro dissolution profile. The mechanistic drug release performance was predicted using the Weibull model (shape factor and lag time) with validation parameters such as (Akaike and criterion parameters) present in HSPiP and GastroPlus. Various tabs of HSPiP needs experimental and theoretical literature based input parameter for simulation and prediction (Wiśniewski et al., 1995).

3.5. Solubility study in various excipients

HSPiP provided various suitable solvents and excipients. The solubility of TM-19 was evaluated in several organic solvents, surfactants, oils and co-surfactants as predicted in HSPiP. In each case, (2 mL) of excipient was transferred to a neat glass vial, followed by an addition of an accurate amount TM-19. The mixture was then placed in a water shaker bath running at 40 °C for 72 h to establish saturation and equilibrium solubility. After 72, the mixture was centrifuged to obtain a clear supernatant and the supernatant and the supernatant was analyzed for drug content. The amount of TM-19 dissolved in each excipient was determined using UV–Vis spectrophotometer (UV 160 1PC, Shimadzu, Japan) at 309 nm. The study was replicated to obtain a mean value.

3.6. GastroPlus based simulation and in-vivo prediction in human for oral delivery

Based on in vitro findings, literature-based data, and default program values (HSPiP and GastroPlus), it was required to predict in vivo performance of the newly synthesized compound TM-19. Oral route of drug delivery is the most preferred among all routes of drug administration. Therefore, this program was used to predict in vivo pharmacokinetic and pharmacodynamics profile in humans. GastroPlus uses ACAT (advanced compartmental and transit) model for simulation in the targeted animal model (Hussain et al., 2022b) [15]. For this purpose, GastroPlus was simulated for 24 h (simulation time) considering a healthy subject of 70 Kg under fast condition to avoid food interaction (version 9.7, Simulation Plus, Inc., Lancaster, United States of America). Known values of physicochemical properties of TM-19 were added to the respective input tabs (compound tab, physiological tab, and pharmacokinetic tab) in GastroPlus. A new option “new pharmacokinetics tab” was used for prediction and simulation. The regional compartmental absorption model predicted percent TM-19 absorption from various gastrointestinal regions (nine compartments). The parameters sensitivity analysis (PSA) assessment of GastroPlus predicted the impact of various critical attributes on prime PK parameters. These PK parameters are (a) area under the curve (AUC), (b) maximum drug concentration reached in the plasma (C_{max}), and (c) the maximum time (T_{max}) required to reach C_{max}.

3.7. Topical formulation as an alternative to oral delivery

3.7.1. Preparation

Various elastic liposomes were prepared using phosphatidylcholine and span 80 in different ratios, following the reported method (Hussain et al., 2020a). In brief, TM-19 (10 mg), and PC were completely dissolved in chloroform (5 mL). Span 80 was separately dissolved in chloroform to get the desired concentrations based on the set ratio. Therefore, span 80 and PC solutions (containing TM-19) were transferred to round bottom flask (RBF) for film formation, which was generated by subjecting to rotary evaporator. The generated film was completely dried to remove chloroform. Then, PBS (phosphate buffer solution at pH 7.4) was used to hydrate the film, resulting in the formation of colloidal suspension as elastic liposomes. Then, elastic liposomes were sonicated (using probe sonicator) for 5 secs with ON/OFF cycles, which reduced the size and produced unilamellar vesicle. Finally, the prepared formulations were kept in freezer for activation overnight.

3.7.2. Characterized parameters

Prepared formulations were characterized for vesicle size, polydispersity index (PDI), zeta potential and entrapment efficiency (%EE). To obtain the vesicle size and PDI values of formulations, samples were diluted using milli-Q water (100 times) and used in zetasizer (Malvern, United State of America). Zeta potential values were estimated without dilution using the same instrument.

3.8. % entrapment efficiency (%EE)

Each formulation (1 mL) was centrifuged (12000 rpm for 10 min) to obtain a pellet at the bottom of centrifuge tube. The supernatant was used to estimate free drug using a UV–Vis spectrophotometer (UV 160, 1PC, Shimadzu, Japan). The experiment was carried out in triplicate to get a mean value.

3.9. Experimental design: Mixture mode

Design Expert® (v.13.07) is an experimental tool used for optimization processes to identify factors, their levels and relative importance. This technique also helps to identify possible interaction between independent variables (factors) and a set of dependent variables (responses) (Hussain et al., 2020b). In this study, a mixture design was used

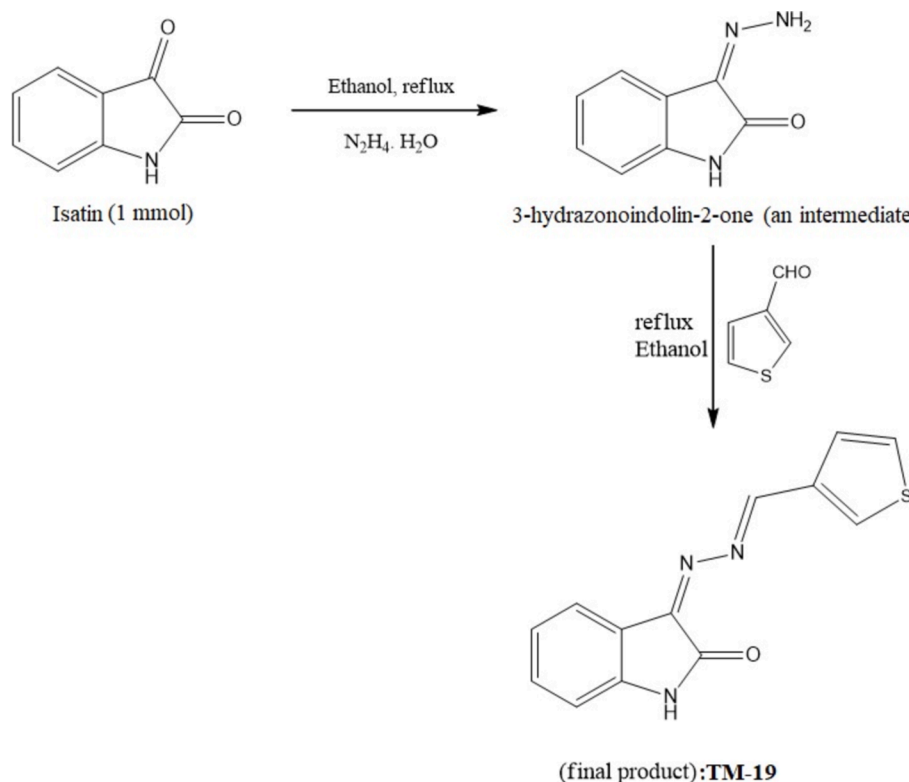


Fig. 1. Scheme 1 for the synthesis of TM-19 (3-((thiophen-3-ylmethylene) hydrazono) indolin-2-one).

by selecting two factors (PC and Span 80). This software helped to identify the significant and non-significant factors during optimization processes. Responses were set to be (Y₁-Y₄) for Vesicle size, PDI, Zeta potential, and % EE, respectively. This technique optimized factors at desired levels to get the most robust formulation as evidenced with several statistical parameters, models and numerical objective functional parameters (desirability). To develop a colloidal suspension containing TM-19 at 2 mg/mL, we used 10 formulations with varying amounts of PC and S80 according to constraints given by the software. Thus, the optimization process suggested the best robust formulation based on the desirability numerical function.

3.10. Thermal analysis: Differential scanning calorimeter (DSC)

DSC for thermal analysis. Amorphous and crystalline states of the samples were evaluated using DSC 4000 (Perkin Elmer Instruments, Shelton, CT, USA) at a scan rate of 20 °C/min. The samples (~3 mg) were weighed and placed in an aluminum pan and lid and was crimped to form a hermetic seal (Sharaby, 2007). Indium was used for calibration (100 % pure, melting point 156.60 °C, heat of fusion 6.80 cal/g). Nitrogen at a rate of 20 ml/min was purged for reference and sample cells.

3.11. Evaluations of formulations

The optimized formulation (TF1) was characterized for vesicle size, PDI, zeta potential, DSC, and morphology using transmission electron microscopy (TEM). The size and size distribution were estimated using zetasizer (Malvern, USA) after 100 times dilution with water. Zeta potential were measured without dilution the sample. TEM was used to scan the sample after loading onto the grid followed by drying and staining (0.1 % phosphatungstic acid). %EE and in vitro dissolution (12 h) studies were performed to estimate % entrapped drug and dissolution performance in PBS solution (900 mL), respectively.

3.12. In vitro cytotoxicity potential of TM-19

TM-19 was potentially active against MCF-7 (at 1 mM molar concentration). Cell culture was conducted as described in our previous work (Alanazi et al., 2020). Briefly, human breast cancer (MCF-7) cell lines were cultured at a density of $\sim 3 \times 10^5$ cells/mL in basal medium containing 1:1 Dulbecco's modified Eagle's medium 1X (DMEM 1X): 10 % fetal bovine serum (FBS): and 1 % streptomycin/penicillin (100 µg/mL and 100 units/mL respectively). Cells were maintained in a humidified incubator containing 5 % of CO₂ at 37 °C. Once cells became confluent, they were passaged by trypsinization (300 µL) into T-75 flasks. All proposed experiments were conducted on cells from passage 19–20. 96 well plates were used for the MTT experiments. All treatments were carried out in full culture medium containing FBS and streptomycin/penicillin. In the presence or absence of variety treatment groups, the medium was changed every other day.

MTT assay (MedChemExpress, the United States of America) is a colorimetric assay used to evaluate either cell proliferation and survival. We evaluated the cytotoxicity of either pure TM-19 suspension, TF1, and TM-19 solution (1 % DMSO) on MCF-7 cells, using the MTT assay as per method reported before (Smirnov et al., 2019). Briefly, cells were cultured as described above. Then, cells were harvested and trypsinized in order to be counted. Furthermore, we seeded 1×10^4 cells per well in 96 well-plates. Following overnight adherence, MCF-7 cells viability was evaluated in cells incubated with either pure TM-19 suspension, TF1, and TM-19 solution (5, 10, 20, and 40 µM) for 24 h. By the end of the experiment, we have added 10 µL of MTT (5 mg/mL in PBS) followed by standing for 60 min. Then, we have added 100 µL of DMSO, while shaking for 5 min. The absorbance was measured by a micro-plate reader at 570 nm. The study was replicated to get mean and standard dedication.

3.13. Statistical analysis

Experiments were replicated (n = 3) to obtain mean, standard error

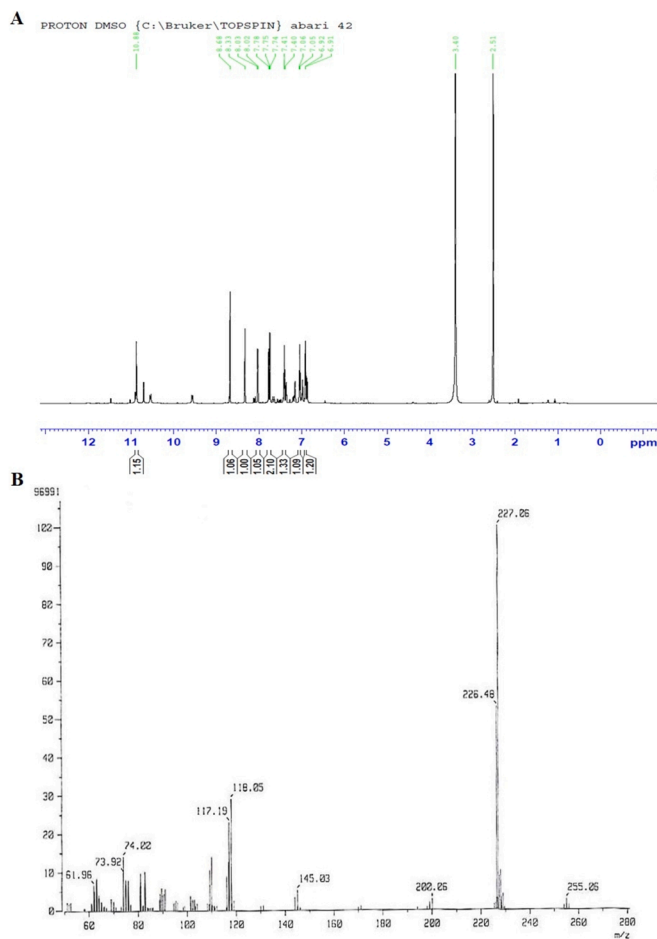


Fig. 2. (A) NMR of the final product and (B) MS for 3-((thiophen-3-ylmethylene) hydrazono) indolin-2-one.

of mean, and standard deviation. In comparison, a value was considered as significant at $p < 0.05$. Microsoft excel (version 16) was used to delineate standard calibration curve and regression analysis ($r^2 \geq 0.99$).

4. Result and discussion

4.1. Synthesis of isatin derivative (TM-19)

To synthesize the intermediate product, 1 mmol of isatin was dissolved in ethanol, followed by the addition of 1.1 mmol of hydrazine hydrate with stirring and a few drops of acetic acid. The reaction mixture was refluxed and, upon completion of reaction, ice was added. The resulting precipitate was filtered, washed with water several times and characterized using ¹H NMR and mass spectroscopic data. In the proton NMR spectra, the peaks at 6.8 – 7.4 ppm represent the aromatic protons, while peaks at 10.9 and 10.6 ppm confirm the presence of NH protons, along with the peak at 9.6 ppm. Equimolar amounts of 3-hydrazonoindolin-2-one and 3-thiophenecarboxaldehyde were dissolved in ethanol with stirring, followed by few drops of acetic acid. The mixture was refluxed, and after completion of the reaction, ice was added. The resulting solid was filtered, washed with water several times, and dried in an oven. The final product TM-19 (Fig. 1) was characterized using NMR and mass spectrometry. In the proton NMR spectrum, no aldehyde and amine protons were observed. Instead, a peak at 11 ppm represents the indole NH group, while aromatic protons appear at their respective positions in proton NMR. ¹³C spectra also confirm the presence of the proposed molecule.

4.2. Nuclear magnetic resonance (NMR)

Yield: 64 %, light yellow solid, MP: 208 °C, IR: $\nu = 1678$ (C = O), 3353 (NH): ¹HNMR (700.170 MHz, DMSO-*d*₆): $\delta = 6.86$ (d, 1H, Ar), 6.98 (t, 1H, I = 14 Hz, Ar), 7.16 (d, 1H, Ar), 7.37 (d, 1H, Ar), 9.56 (d, 1H, I = 14 Hz, NH-H), 10.55 (d, 1H, J = 14 Hz, NH-H), 10.69 (brs, 1H, N). ¹³C NMR (176.07 MHz, DMSO-*d*₆): $\delta = 110.4$, 117.92, 121.83, 122.72, 126.66, 127.51, 139.10, 163.24. MS (ESI, 70 eV): m/z 161 (M + H)⁺, 104. Anal. Calcd. for C₈H₇N₃O.

Yield: 60 %, dark red solid, MP: 210°C IR: $\nu = 1778$ (C = O), 3278 (NH): ¹HNMR (700.170 MHz, DMSO-*d*₆): $\delta = 6.91$ (d, 1H, Ar), 7.05 (t, 1H, Ar), 7.40 (t, 1H, Ar), 7.74 (dd, 2H, Ar), 8.02 (1H, CH), 8.33 (s, 1H, Ar), 8.68 (s, 1H, Ar), 10.87 (br s, 1H, NH). ¹³C NMR (176.07 MHz, DMSO-*d*₆): $\delta = 111.25$, 117.04, 122.87, 125.80, 129.06, 129.51, 134.09, 134.11, 137.54, 145.37, 151.35, 157.10, 165.13. MS (ESI, 70 eV): m/z 161 (M + H)⁺, 255.05. Anal. Calcd. for C₁₃H₉N₃O (Fig. 2A of Fig. 2).

4.3. Mass spectroscopy of the synthesized compounds

The mass spectra of the final product showed the molecular ion peak at 255, along with the base peak at 227, which confirm the presence of the proposed molecule (Fig. 2B).

The mass spectrometry data strongly corroborates and extends the structural insights gained from NMR analysis of TM-19. The molecular ion peak at m/z 255 confirms the molecular formula C₁₃H₉N₃O, consistent with the 13 carbon signals observed in the ¹³C NMR spectrum and the incorporation of the thiophene ring. This odd-numbered molecular mass verifies the presence of three nitrogen atoms, supporting the rearrangement of nitrogen atoms inferred from the NMR data, where we observed a reduction from three N–H signals in the intermediate compound to one in TM-19. The intense molecular ion peak indicates a stable system, aligning well with the NMR data suggesting a structure combining benzene and thiophene rings. Furthermore, the mass spectrometry data confirms the thiophene incorporation, corroborating the NMR signals attributed to thiophene protons (singlets at δ 8.33 and 8.68 in ¹H NMR) (Sharaby et al., 2007).

The base peak at m/z 227 in the mass spectrum suggests the loss of CO (28 mass units) from the molecular ion, consistent with the presence of a carbonyl group identified in both the IR spectrum (1725 cm⁻¹) and the ¹³C NMR (likely the signal at δ 165.13). The combined analysis gives us a high degree of confidence in the proposed structure of the final product and offers valuable insights into its chemical properties and reactivity. It confirms not only the structural components identified through NMR but also provides additional information about the molecule's stability and potential fragmentation behavior, which can be crucial for understanding its chemical characteristics and potential applications (Fig. 2B of Fig. 2).

4.4. ATR-FTIR of TM-19

To assess the IR spectra, 5 mg of the samples (intermediate and TM-19) were dissolved in ethanol and dropped onto the ATR crystal surface for drying. Once completely dried, samples were scanned under using ATR-FTIR (ATR-FTIR, Bruker Alpha, Germany). Each sample was scanned 16 times between 4000 and 400 cm⁻¹ to identify stretching and vibration related to the functional groups of TM-19. The band around 3200 cm⁻¹ represents the NH group, while the sharp peak at 1725 confirms the presence of C = O group in the structure (Fig. 3A-B).

To assess the IR spectra, 5 mg of the samples (intermediate and TM-19) were dissolved in ethanol and dropped onto the ATR crystal surface for drying. Once completely dried, samples were scanned under using ATR-FTIR (ATR-FTIR, Bruker Alpha, Germany). Each sample was scanned 16 times between 4000 and 400 cm⁻¹ to identify stretching and vibration related to the functional groups of TM-19. The significant shift in the C = O peak from the intermediate (1678 cm⁻¹) to TM-19 (1725 cm⁻¹) indicates a major change in the carbonyl environment,

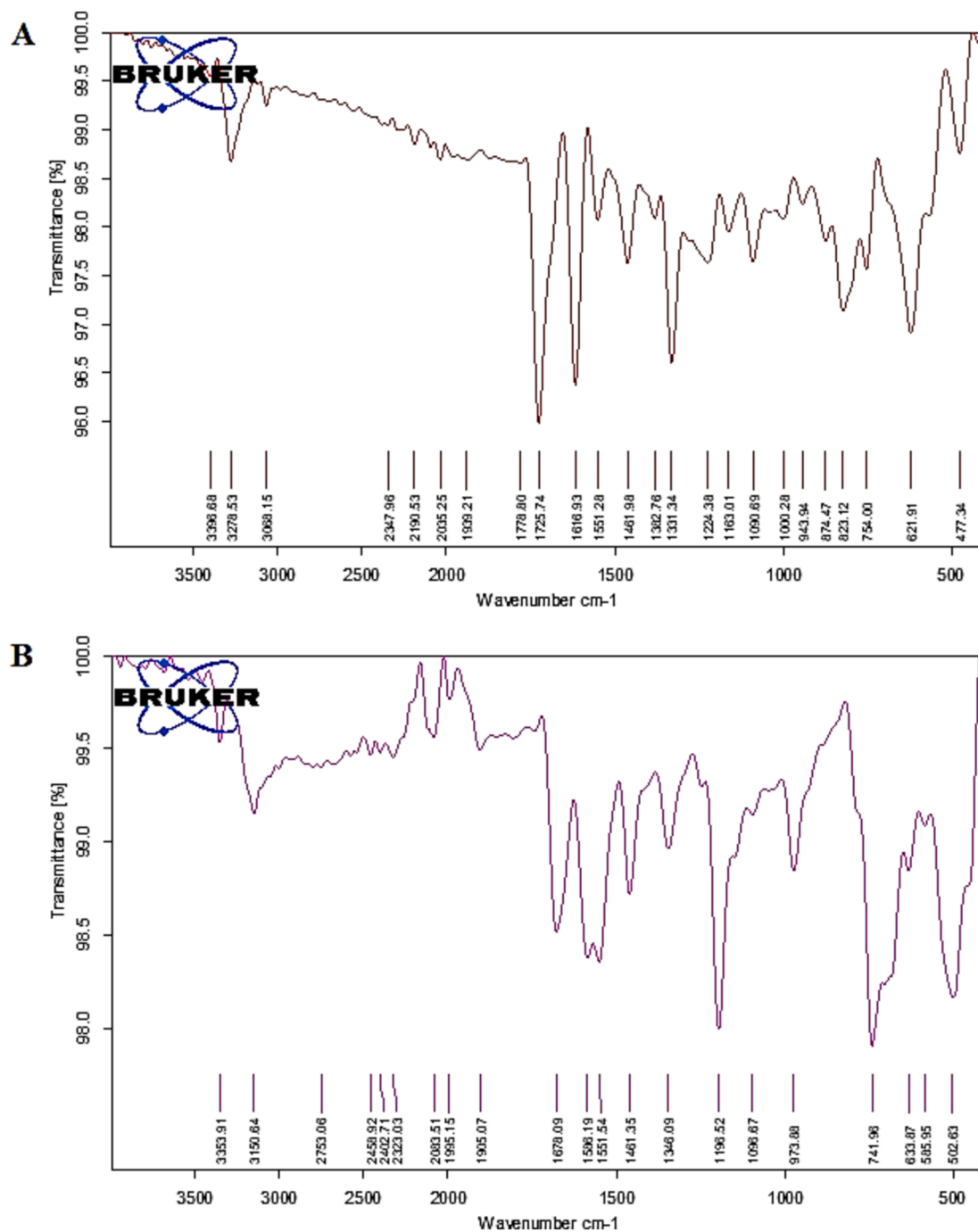


Fig. 3. FTIR: (A) intermediate and (B) final product TM-19.

Table 1
System suitability of 3-((thiophen-3-ylmethylene) hydrazono) indolin-2-one.

Conc. ppm	Area (a.u.)	Retention times (min.)
50	866,024	2.507
50	883,343	2.508
50	840,195	2.511
50	846,616	2.511
50	872,420	2.512
50	870,379	2.516
Mean	863162.8	–
STDEV	16459.12	–
RSD (%)	1.91	–

consistent with substantial structural modifications. This shift strongly supports the formation of a structure involving a Schiff base, as inferred from the other spectroscopic data. The high C = O frequency could indicate its incorporation into a strained cyclic system or proximity to electron-withdrawing groups, which aligns with the proposed structure involving aromatic and thiophene systems evidenced by NMR and mass spectrometry. While the FTIR data doesn't directly confirm the presence of the aromatic and thiophene rings, these structural features would contribute to the electronic environment causing the high C = O frequency. This comprehensive spectroscopic analysis provides robust confirmation of the proposed structure for TM-19, including the Schiff base formation and thiophene incorporation. The band around 3300 cm⁻¹ represents the NH group. The aromatic and thiophene (C–H vibration) would typically show bands in the ~ 3200 cm⁻¹ region (Smirnov et al.,

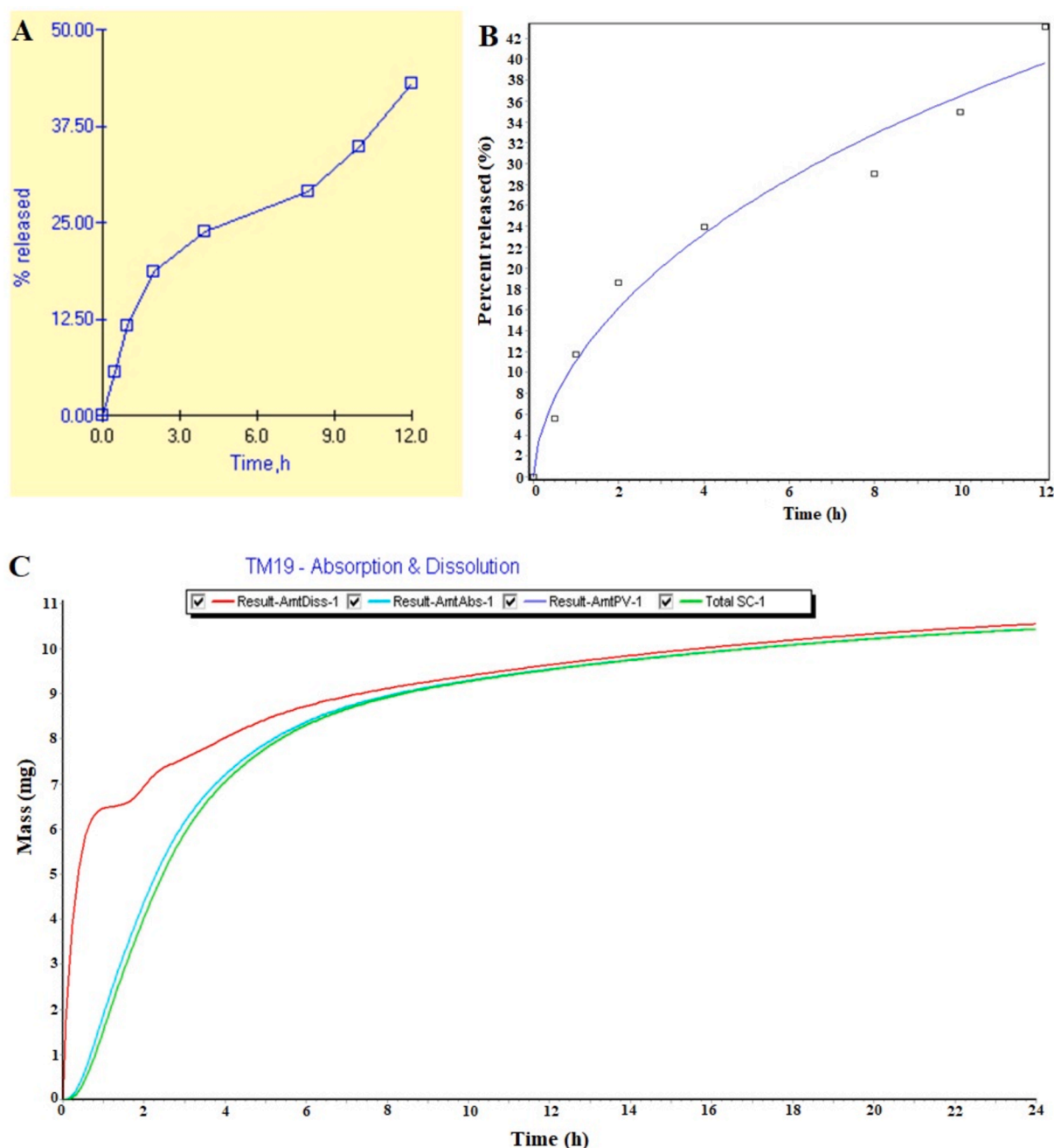


Fig. 5. GastroPlus based simulation and prediction of dissolution in human (fasted condition). (A) Experimental dissolution profile of TM-19 in phosphate buffer solution at pH 6.8, (B) in vitro dissolution and simulation using Weibull model of GastroPlus program, and (C) Predicted in vivo dissolution and in vivo absorption of TM-19 (considering suspension in formulation tab) for a period of 24 h of simulation time in GastroPlus. The value of β was 0.58 which suggests the release mechanism of TM-19 from oral suspension while dissolution followed Fick's diffusion ($\beta \leq 0.75$) [28].

the peak resolution for our compound of interest were more than 1.5, indicating good separation between peaks. The relative standard deviation of six injections was 1.9 %, indicating good precision and reproducibility of the method. These results confirm that the developed method is suitable for the analysis for our compound of interest.

4.7. Linearity

The linearity of 3-((thiophen-3ylmethylene) hydrazono) indolin-2-one was determined from the standard concentrations ranging from 1–100 ppm/ml. The peak intensity versus concentration calibration curve was created, and the correlation coefficient and regression line equation were calculated (supplementary figure S2).

4.8. Precision

To determine the precision of the developed method, six injections were performed individually at three different concentrations (5.0 ppm, 50 ppm, and 100 ppm). The % recoveries were calculated and found to fall between approximately 98–102 %. These results indicate that the developed method is precise and can accurately recover the compound of interest at different concentrations. Table 1 summarized data of system suitability.

Precision (intermediate) ruggedness: To evaluate the intraday analysis of the standard solutions, the linearity curve was calculated. The means of the linearity curve were found to be in the range of 99.6 % to 100.25 %, indicating good accuracy of the developed method. The

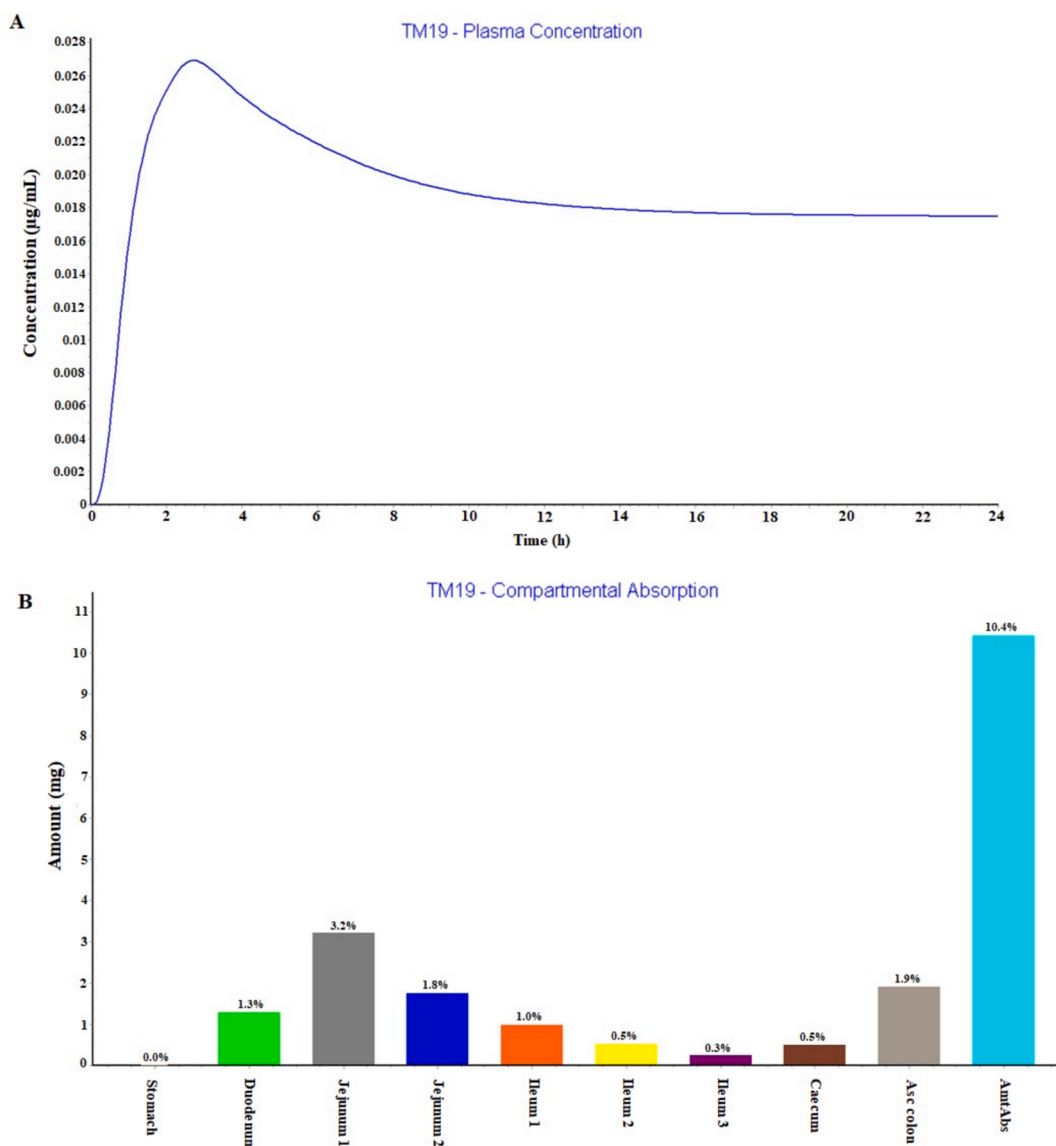


Fig. 6. (A) GastroPlus based predicted plasma concentration time profile in human for 24 h in fast condition and (B) Regional compartmental absorption of TM-19 from nine segments of human gastrointestinal tract.

relative standard deviation (RSD) range was found to be between 1.2 % to 1.6 %, indicating good precision and reproducibility of the method. These results confirm the reliability of the developed method for the analysis of the compound of interest.

Specificity: Specificity also performed, we have run the solution of 3-((thiophen-3ylmethylene) hydrazono) indolin-2-one spiked with both starting materials and all peaks were resolved perfectly fine with more than 1.0 resolution.

Limit of detection: The lowest quantity or concentration of a component that can be reliably detected with a given analytical method. We calculated using the linear curve and found to be 4.20 ppm (lower limit of detection, LLOD).

Limit of quantification: Limit of quantification is the lowest concentration of the analyte that can not only be detected but can be quantified within defined limits, and calculated to be 12.75 ppm (lower limit of quantification, LLOQ).

4.9. HSPiP software based prediction of HSP in various solvents

HSPiP program is a versatile application used in various industries, including paint, drug delivery, and chromatographic method

development and validation. HSPiP is based on the concept of cohesive energy (including solid surface energy) in compounds, which is the sum of various individual energies. Therefore, the total cohesive energy of a solute or a solvent is distributed over dispersion energy, polarity energy, and hydrogen bonding energy (Owens and Wendt, 1969). HSPiP uses HSP which include dispersion parameter (δ_d), polarity parameter (δ_p), and hydrogen bonding parameter (δ_h) for a solute or solvent at particular temperature. In literatures, many researchers established and claimed a direct correlation between the surface energy of a solute and the solubility parameters (HSP) for improved interaction and solubility (Zisman, 1963; Comyn, 1997; Wiśniewski et al., 1995; Altamimi et al., 2016; Alanazi et al., 2020; Alqahtani et al., 2022).

HSPiP predicts various physicochemical, thermodynamic, diffusion coefficients, permeation flux, a time required to saturate a polymer, and solubility model related parameters. Moreover, HSPiP classifies solvents in two different categories, bad or good, based on the estimated value of RED (relative energy difference). The HSP values of HSPiP can be used to screen suitable solvents for drug solubility/miscibility during pre-formulation development, thereby shortening new formulation development duration, reducing product cost and accelerating new drug approval time. HSPiP was previously used in developing green

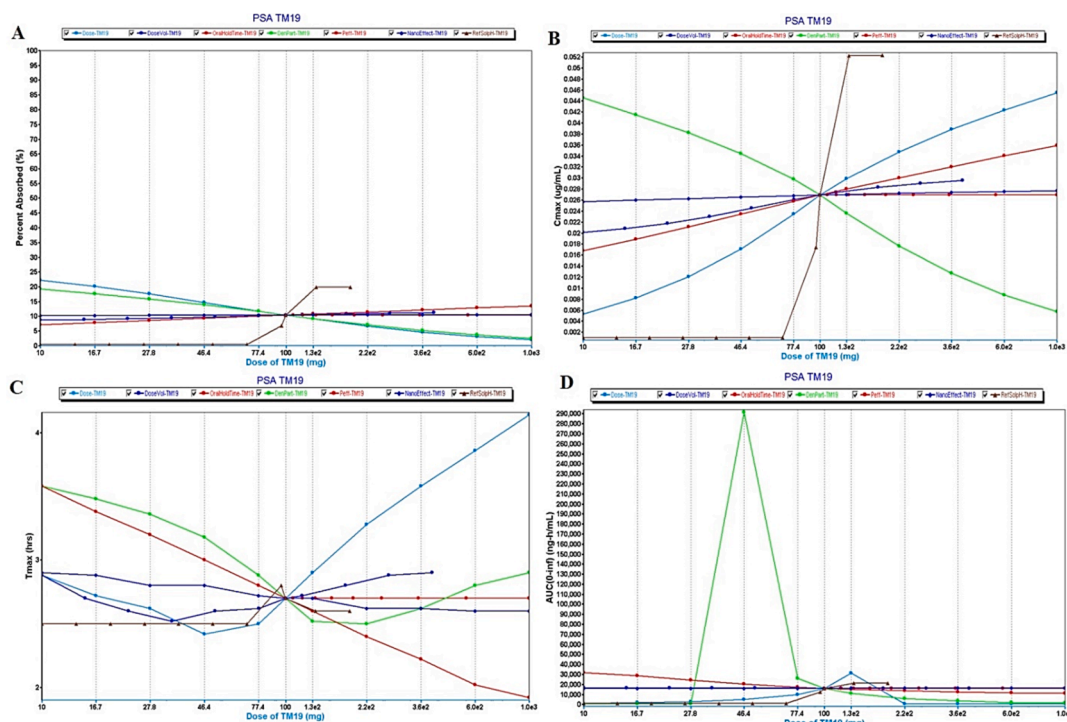


Fig. 7. Parameter sensitivity analysis (PSA) assessment of GastroPlus. (A) impact of various factors on percent drug absorption of TM-19 after oral delivery (fast condition), (B) various factors affecting C_{max} in human (fast), (C) Critical factors affecting T_{max} in human, and (D) Impact of various factors on $AUC_{(0-\infty)}$ in human as predicted in GastroPlus prediction and simulation program.

Table 4

Summary of GastroPlus based predicted pharmacokinetic profiles of TM-19 suspension after oral delivery.

Pharmacokinetic parameters	Predicted value in GastroPlus
C_{max} (µg/mL)	0.0269
$AUC_{(0-\infty)}$ (µg.h/mL)	16.099
$AUC_{(0-4)}$ (µg.h/mL)	0.4553
T_{max} (h)	2.72
Liver C_{max} (µg/mL)	0.4879
Fa (%)	10.43

nanoemulsion to control water contamination, selection of various excipients for a formulation development intended for topical application, and UPLC method development by optimizing the mobile phase using HSP values (Hussain et al., 2022a; Altamimi et al., 2016; Alanazi et al., 2020). Thus, it is interesting to apply HSPiP program to select an appropriate organic solvent for TM-19 and compare the predicted solubility to the experimental solubility in the selected solvents. The result of the estimated HSP values for TM-19 and various solvents are summarized in Table 2. The values of δ_d , δ_p , and δ_h and δ for TM-19 are 20.2, 11.0, 3.9, and 23.5, respectively as predicted in HSPiP. The calculated values of RED for the predicted solvents are provided in Table 2, where glycerol and chloroform exhibit the highest and lowest values, respectively. Therefore, HSPiP predicted the highest solubility of TM-19 in chloroform and the lowest in glycerol at 25 °C. The lowest solubility of TM-19 in glycerol may be attributed to its inability to form hydrogen bonding with glycerol as evidence with the large difference (~ 24) in δ_h values between the solute and the solvent in HSPiP program (Hansen, 2007; Abbott, 2012).

4.10. Solubility study in various HSPiP based predicted excipients

Based on the HSP values (estimated from (HSPiP) of TM-19 and the explored solvent, it was predicted that glycerol is not suitable for TM-19

solubility whereas chloroform was supposed to execute good solubility. Therefore, experimental solubility of TM-19 in the predicted solvent was necessary. The experimental solubility of TM-19 in various HSPiP based predicted excipients, was conducted, and the results are presented in Fig. 4. HSPiP predicted that TM-19 would be most soluble in chloroform among the selected solvents. However, TM-19 was highly lipophilic and the maximum solubility was obtained in DMSO (19.3 ± 1.3 mg/mL) than chloroform. This finding may be correlated to the HSP values of TM-19, which were closer to DMSO than chloroform (as predicted in HSPiP). The difference values of $\Delta\delta_d$ (δ_d of TM-19 – δ_d of DMSO = 1.8) and $\Delta\delta_p$ (δ_p of TM-19 – δ_p of DMSO = 3.6) are significantly low than the $\Delta\delta_d$ (2.6) and $\Delta\delta_p$ (5.2) values of chloroform based on predicted values (HSPiP). HSPiP based prediction was consistent with the other solvents. Water and ethyl acetate exhibited no solubility, which may be due to drug's lipophilic nature and lack of interaction with polar solvents which was consistent with the predicted outcome of HSPiP. Chloroform showed good solubility, second to DMSO, and therefore, TM-19 was solubilized first in chloroform to formulate elastic liposomes formulations.

4.11. GastroPlus based predicted oral pharmacokinetic profile of TM-19

In order to determine simulation behavior of in vitro dissolution data and predictive in vivo dissolution performance more accurately, the generated in vitro dissolution data of TM19 suspension was directly fed in the respective tab of in silico model (Wang et al., 2021; Kesharwani and Ibrahim, 2023; Ni et al., 2017). Based on experimental data obtained from in vitro studies, the predicted pharmacokinetics parameters, in vivo dissolution and absorption, and predicted regional absorption values were found to be quite interesting and convincing. As expected from the experimental solubility data, HSPiP based predicted Hansen parameters were simulated with significant correlation. TM-19 was highly insoluble in water ($\log P = 3.2$) (Table 3). Various predicted physicochemical properties (HSPiP) of TM-19 were found to be consistent with the experimental values (experimental and literature).

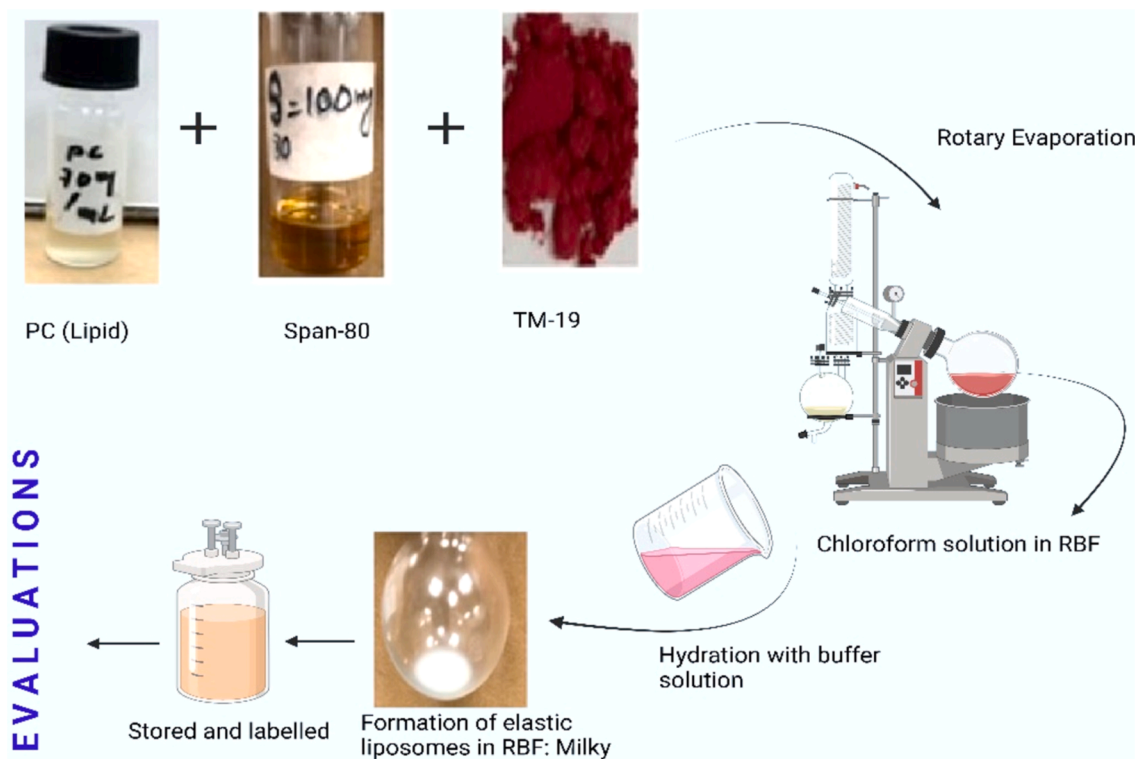


Fig. 8. Schematic representation of adopted method for the preparation of elastic liposomes.

Table 5
Summary of composition of various formulations as per the suggested model.

Std	Run	Factors		Responses			
		X ₁ (mg) A: PC	X ₂ (mg) B: Span 80	Y ₁ (nm)	Y ₂ (PDI)	Y ₃ (mV)	Y ₄ (% EE)
1	1	92.5	7.5	469 ± 12.7	0.39 ± 0.03	-11.5 ± 1.5	57.3 ± 5.5
5	2	88.75	11.25	406 ± 10.4	0.52 ± 0.08	-13.0 ± 2.2	40.06 ± 7.8
8	3	92.5	7.5	447 ± 19.8	0.42 ± 0.02	-10.8 ± 1.6	56.0 ± 9.2
2	4	77.5	22.5	348 ± 9.1	0.48 ± 0.06	-12.9 ± 2.7	62.9 ± 11.9
7	5	85.0	15.0	850 ± 23.7	0.66 ± 0.11	-11.5 ± 0.9	57.3 ± 10.5
3	6	87.5	12.5	418 ± 15.5	0.32 ± 0.02	-10.2 ± 1.7	50.7 ± 8.4
6	7	81.25	18.75	697 ± 19.0	0.56 ± 0.06	-12.6 ± 1.8	49.8 ± 3.8
10	8	92.5	7.5	472 ± 13.2	0.36 ± 0.03	-11.8 ± 2.3	52.7 ± 7.1
9	9	77.5	22.5	360 ± 10.9	0.43 ± 0.05	-13.1 ± 2.1	60.4 ± 9.9
4	10	82.5	17.5	709 ± 19.4	0.63 ± 0.09	-12.0 ± 1.5	49.0 ± 6.3
The sets of constraints for the model							
Low limit		Constraints				High limit	
77.500	≤	A: PC	≤			92.500	
7.500	≤	B: Span 80	≤			22.500	
		A + B	=			100.00	

Therefore, GastroPlus based predicted in vivo dissolution was low and subsequently limited absorption (Fig. 5A-C). Fig. 5A exhibited experimental solubility of TM-19 in buffer (pH 7.8) whereas Fig. 5B revealed GastroPlus based Weibull model fit for simulation (suggested diffusion

based drug release/dissolution). Fig. 5C illustrated in vivo dissolution of TM-19 as predicted in the program.

Fig. 6A and 6B illustrated plasma drug concentration time profile for TM-19 suspension humans over period of 24 h and regional compartmental absorption of TM-19 from various regions of GIT, respectively as predicted in GastroPlus. The overall oral absorption was 10.4 % which may be due to lipophilic nature of TM-19. Moreover, TM-19 absorption was primarily from upper GIT regions except stomach (duodenum and jejunum) as predicted in GastroPlus. PSA assessment report of GastroPlus predicted that dose, dosing volume, nanoEffect, reference solubility, apparent permeability coefficient, oral hold time, and particle density had remarkable impact on major pharmacokinetic parameters such as T_{max} , C_{max} , and AUC (area under the curve) (Fig. 7A-D). Thus, these predicted values suggested that the synthesized compound TM-19 is not suitable for oral delivery due to highly lipophilic nature and limited in vivo absorption in humans as predicted in GastroPlus program. Table 4 summarized various GastroPlus based predicted PK parameters for TM-19 considering oral route of drug delivery in solid dosage form.

4.12. Topical elastic liposomes preparation and characterized parameters

4.12.1. Preparation and pre-optimization

To prepare the formulations, a general rotary film evaporation method was employed, and the steps involved are depicted in Fig. 8. A fixed amount of TM-19 was used in all formulations to optimize the range of PC and span-80 for expected stability. Based on benchtop stability, the maximum and minimum values of each primary excipient (PC and span 80) were determined and used in the experimental design (Hussain et al., 2017). A total ten formulations were suggested and are presented in Table 5 under set conditions of constraints (Table 1 and Table 4). All formulations were stable over night at room temperature without any signs of physical instability, such as drug precipitation and phase separation.

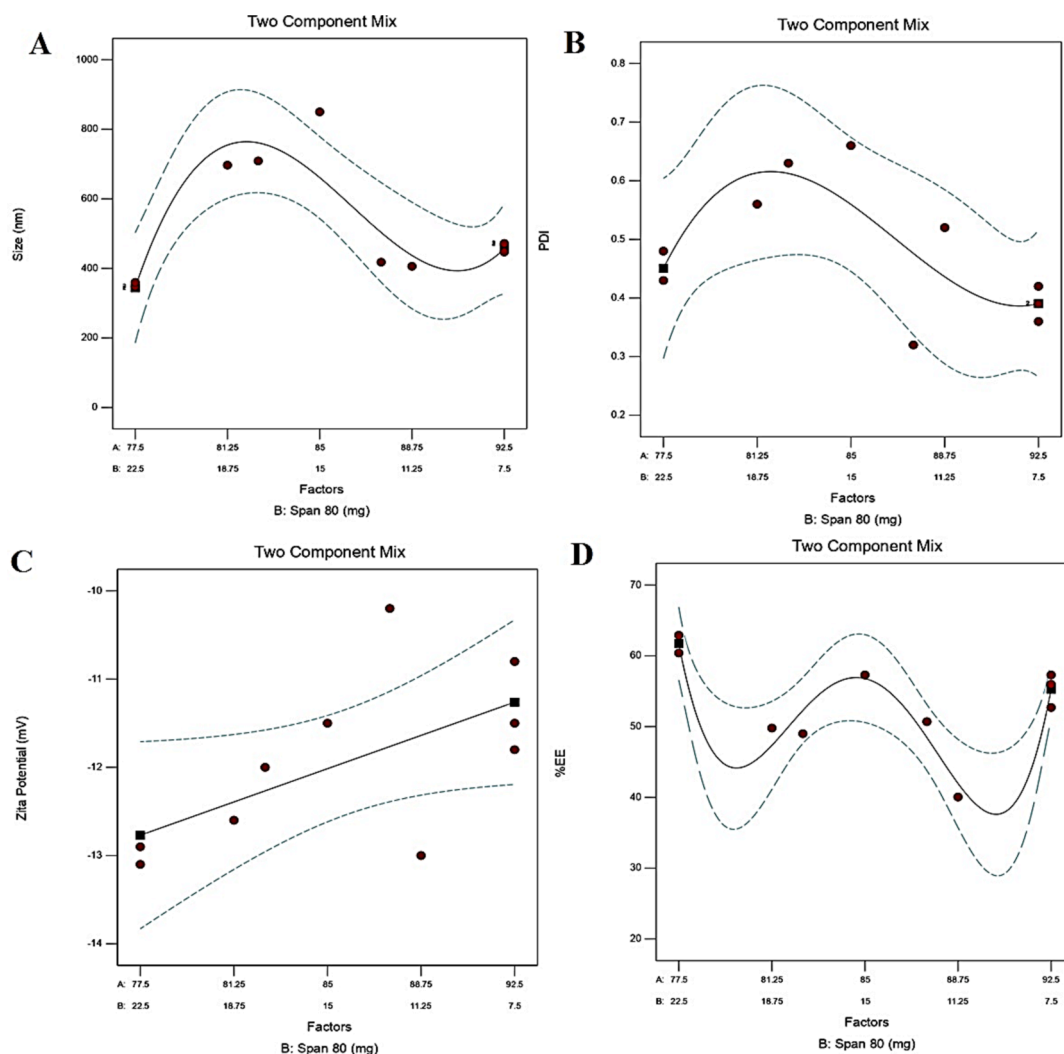


Fig. 9. Independent and dependent variables in mixed design.

4.13. Optimization using experimental design: Mixture mode

In the mixed design, two factors were processed against four responses (Y_1 - Y_4), and the results are presented in Fig. 9 and Table 6 (Snee, 1971). The response Y_1 , Y_2 , Y_3 , and Y_4 were processed considering at a minimum, in-target, and maximum goal, respectively. A cubic model was found to be the best fit for response Y_1 and Y_2 . Linear and quartic models were found to be the best fit for responses Y_3 , and Y_4 , respectively. The two-dimensional response plot for each response is illustrated in Fig. 9. The finally optimized and suggested formulation needs to be reformulated and characterized for vesicle size, PDI, zeta potential and %EE. Based on the results, a conclusive result can be proposed by comparing predicted and experimentally obtained findings. Other parameters, such as in vitro drug release, morphological studies, and interaction investigations are being pursued. Recently, we established HSPiP and QbD based analytical methodology for efficient and reproducible analysis (Altamimi et al., 2022).

4.14. Desirability as numerical function parameter

The desirability function parameter is a numerical function used to validate the optimization using design expert. Its value varies from zero to unity, suggesting the best fit of the model under given set of constraints and importance (Hussain et al., 2022b). The most robust formulation was suggested with a desirability function value of 0.974, as

shown in Fig. 10 (Altamimi et al., 2021b). The bar graph showed maximum desirability of 0.974 (overall desirability). Individual desirability values for Y_1 , Y_2 , Y_3 , and Y_4 were 1, 1, 1, and 0.94, respectively.

4.15. Differential scanning calorimetry (DSC)

The thermal behavior of TM-19, PC, PM, and TF-1 was studied using DSC. This analysis revealed a broad melting peak for TM-19 (as T-19) of 155 °C as shown in Fig. 11. A single endothermic peak was found for PC at peak temperature of 124 °C. Physical mixture and formulation showed melting temperature around 120 °C. However, melting peak of TM-19 was not detected in the formulation indicating a transformation of the crystal form to the amorphous counterpart and the absence of the crystalline state of the drug in the delivery system (Vanessa et al., 2011).

4.15.1. Characterized parameters

All ten formulations were characterized for vesicle size, PDI, zeta potential and %EE, and results are presented in Table 5. It is evident that each formulation showed a negative zeta potential due to the lipid content in composition (Wang et al., 2020). There was no significant change in zeta potential values among formulations due to insignificant lipid variation in the formulation. Vesicular size varied according to the lipid and span 80 contents. With an increase in PC with respect to span 80, the vesicles size was found to be increased and vice versa (Yanar et al., 2020). Formulations containing PC > 80 % revealed a size greater

Table 6
Summary of the model in QbD based optimizations and statistical data.

Model coefficients	Responses			
	Y ₁	Y ₂	Y ₃	Y ₄
A	456.76	0.3905	-11.26	55.28
B	344.11	0.4504	-12.77	61.74
p-value	0.7259	0.1585	0.0605	+0.5515
F-value	0.1351	2.59	4.77	
AB	1042.91	0.5570	-	-6.88
p-value	0.0085	0.0786	-	0.1631
F-value	14.79	4.48	-	2.52
AB(A-B)	-1992.8	-0.7855	-	-268.00*
p-value	0.0142	0.2143	-	0.0078*
F-value	11.68	1.93	-	18.45*
Model Statistics				
r ²	0.8085	0.5924	0.3734	0.8978
Adjusted r ²	0.7127	0.3886	0.2950	0.8161
Predicted r ²	0.5724	-0.1313	0.1521	0.4428
Model p-value	0.0142	0.1232	0.0605	0.0108
Model F-value	8.44	2.91	4.77	10.99
Observed/(predicted) Values				
Optimized	Y ₁	Y ₂	Y ₃	Y ₄
TF1	(344.11, (X ₁ = 77.5 and X ₂ = 22.5 mg)	(0.45)	(-12.77, mV)	(61.741, %)
Polynomial Equations for Each Response				
	Y ₁ = 27.20X ₁ - 7530.53 X ₂ + 128.62 X ₁ X ₂ - 0.590 X ₁ X ₂ (X ₁ -X ₂)			
	Y ₂ = 0.011X ₁ - 3.01 X ₂ + 0.051 X ₁ X ₂ - 0.0002 X ₁ X ₂ (X ₁ -X ₂)			
	Y ₃ = -0.105 X ₁ - 0.2056 X ₂			
	Y ₄ = 8.783X ₁ - 10929.52 X ₂ - 206.706 X ₁ X ₂ + 1.479 X ₁ X ₂ (X ₁ -X ₂) - 0.0053 X ₁ X ₂ (X ₁ -X ₂) ²			

* Indicate the term is (AB(A-B)²) because the term (AB(A-B)) is not significant.

than 400 nm, whereas formulations containing PC below 80 % resulted in a size lower than 400 nm. This indicates that a proper ratio of PC to span 80 is required to obtain the most robust formulation with expected responses and high desirability. Similar pattern was observed in PDI values (Table 5). Fig. 12 illustrated the vesicle size, zeta potential, and TEM morphology of the optimized TF1, respectively.

4.16. % entrapment efficiency (%EE)

TM-19 was highly lipophilic and it was expected to be entrapped in the lipid bilayer of the vesicles (Gulati et al., 1998). However, there are other factors that control %EE. The results of %EE are presented in Table 5 and the table showed that formulations containing the lowest PC content and high span 80 resulted in high %EE, whereas low span 80 with respect to PC caused insufficient vesicle formation after hydration and subsequently poor stability. A low content of span 80 is unable to form stable and firm vesicles, and there are probable chances of drug leakage during storage. Span 80 is capable to perturb and hemifuse with the PC lipid bilayer and may cause leakage at low concentration (Corsaro et al., 2021; Hayashi et al., 2013).

4.17. In vitro cytotoxicity study

Various isatin derivative have been reported in the literature for potential activity against breast cancer (Chauhan et al., 2022; Chowdhary et al., 2022; Zhao et al., 2023). The result of cytotoxicity study is illustrated in Fig. 13. TM-19 was found to have potential cytotoxicity (51.5 % inhibition) against MCF-7 at 10 μM concentration (Fig. 13A). However, the product had no convincing effect against other cell lines such as MDA-MB-231/ATCC, HS 578 T, BT-549, T-47D, and

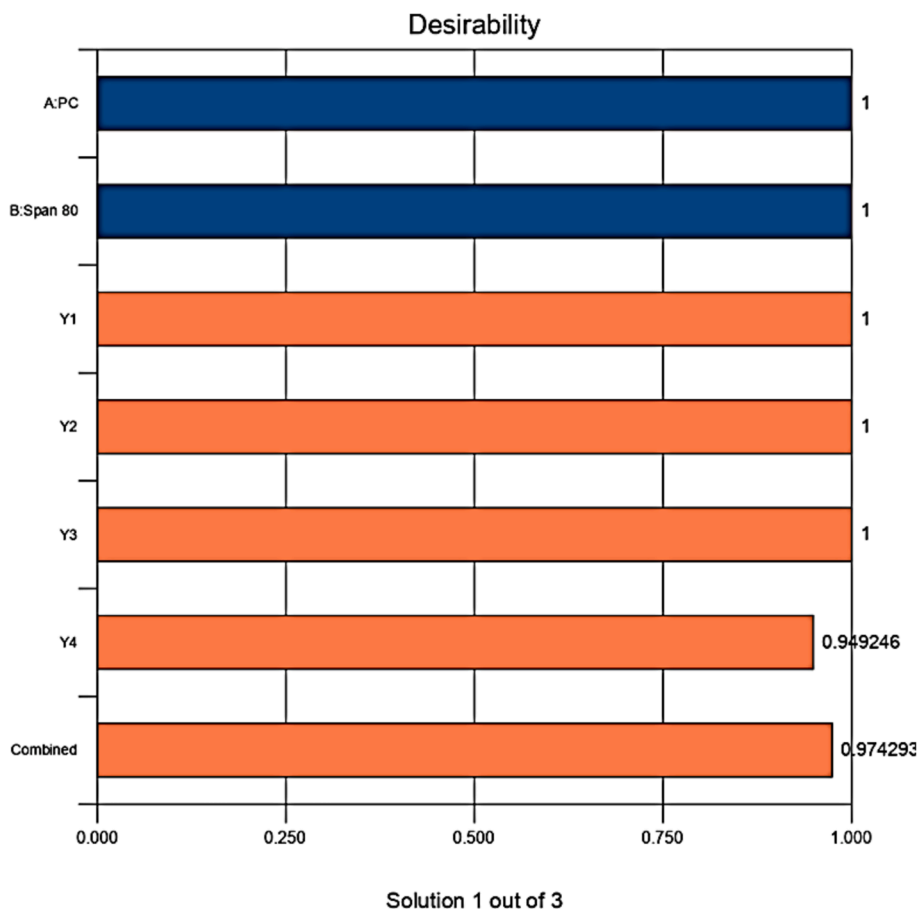


Fig. 10. Overall desirability bar graph and individual desirability of each factor and response.

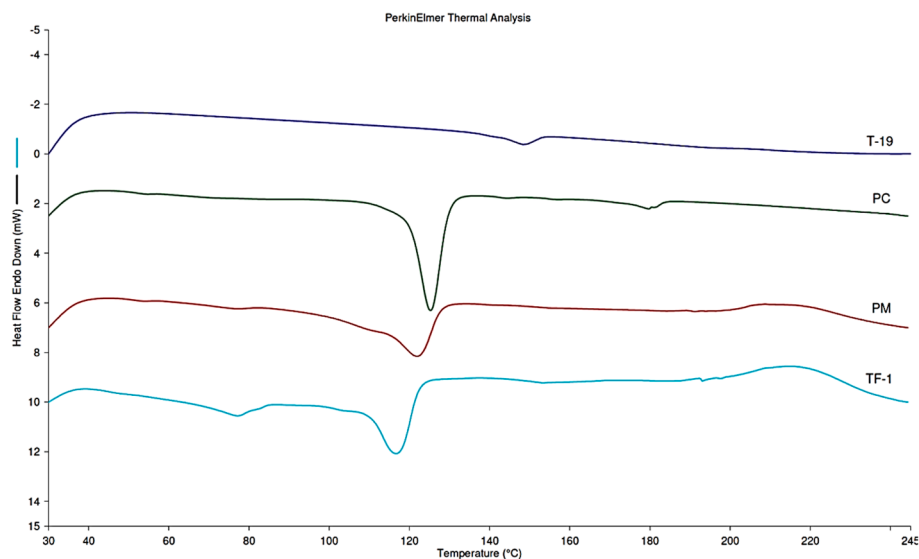


Fig. 11. Thermograms for TM-19, PC, physical mixture, and trial formulation (TF-1).

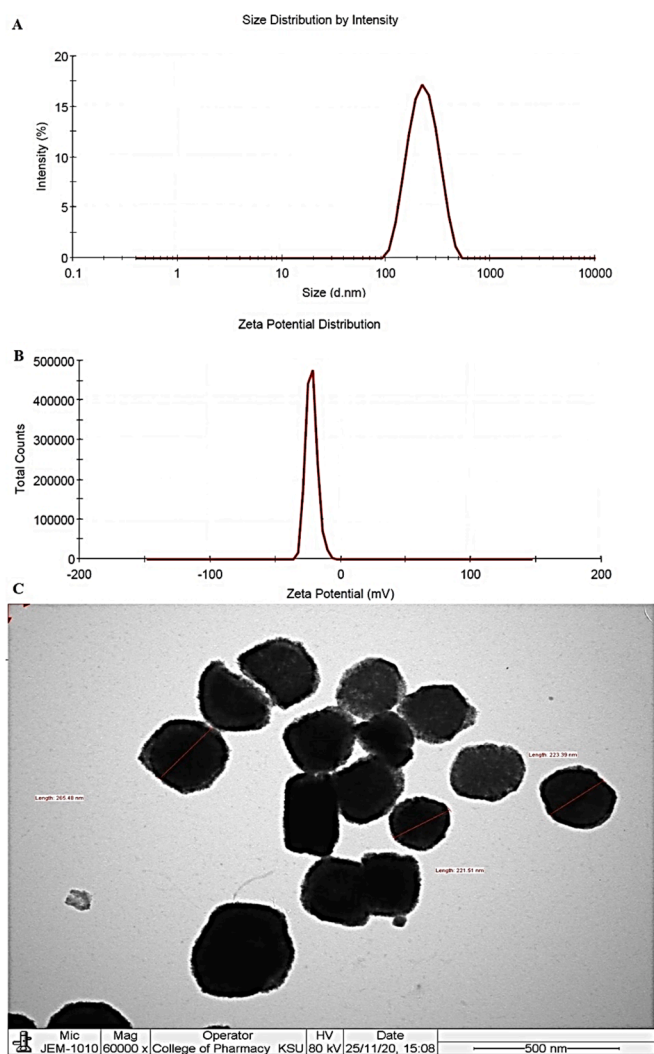


Fig. 12. Evaluated parameters of the optimized TM-19 loaded elastic liposomes (TF1). (A) Vesicle size distribution, (B) Zeta potential, and (C) representative photomicrograph of transmission electron microscopy at 60000X magnification and 80 kV voltage.

MDA-MB-468. TM-19 suspension, TF1, and TM-19 solution substantially reduced the viability of MCF-7 cells as compared to the control group (Fig. 13b). Notably, TM-19 and formulations exhibited dose-dependent decreased viability of MCF-7 cells as compared to the control group (5 μM ; 26 %; $P < 0.0001$, 10 μM ; 55 %; $P < 0.0001$, 20 μM ; 89 %; $P < 0.0001$, and 40 μM ; 91 %; $P < 0.0001$) (Fig. 13C and Fig. 13D). In TF1, the outcome was quite convincing due to significant reduction at all explored concentration ranges (5 μM ; $P < 0.001$, 10 μM ; $P < 0.01$, 20 μM ; $P < 0.05$, and 40 μM ; $P < 0.0001$). Interestingly, both TF1 and TM-19 solution have showed marked declined in the viability of MCF-7 cells in a dose-dependent manner such as 5 μM (67 %; $P < 0.0001$), 10 μM (90 %, $P < 0.0001$), 20 μM (94 %, $P < 0.0001$), and 40 μM (94 %; $P < 0.0001$) as compared to the previous group and the control. In this study, we tailored negatively charged elastic liposomes to inhibit in vitro vesicular aggregation and enhanced liposomes stability followed by expected enhanced cellular uptake, decreased leakage of the loaded drug from the vesicles as compared to positively or neutral lipid based elastic liposomes (Hussain et al., 2014). The obtained potential activity of TM-19 and related formulation may be attributed to isatin-induced MCF-7 cytotoxicity through modulation of apoptosis pathway (Ma et al., 2014; Chauhan et al., 2022). Interestingly, another study highlighted that the anti-breast cancer activity of isatin is not limited to the pure compound. However, many newer isatin analogue similar to TM-19 were even more effective against many different breast cancer cell lines, including MCF-7 (Ma et al., 2014; Chauhan et al., 2022). Similarly, Guo et al. reported a newly synthesized isatin analogue with potential cytotoxic activity against broad range of breast cancer cell lines, including: MCF-7 (Guo et al., 2020). For further exploration, a targeted functionalized derivatization or ligand based functionalized elastic liposomes can be recommended to improve in vivo pharmacokinetics in animal model as reported in various literature (Alhariri et al., 2017). Furthermore, our findings confirm that TM-19 has potential anti-breast cancer activity which can be further explored for in vivo performance in a suitable animal model.

5. Conclusion

Our findings encourage the potential implementation of TM-19 in cancer treatment. The synthesized molecules could further be derivatized and modified for maximum potency and less toxicity. Here, TM-19 was characterized and confirmed for structural identification using mass spectroscopy and NMR. Oral route of administration is the most preferred over others. Therefore, GastroPlus predicted various in vivo

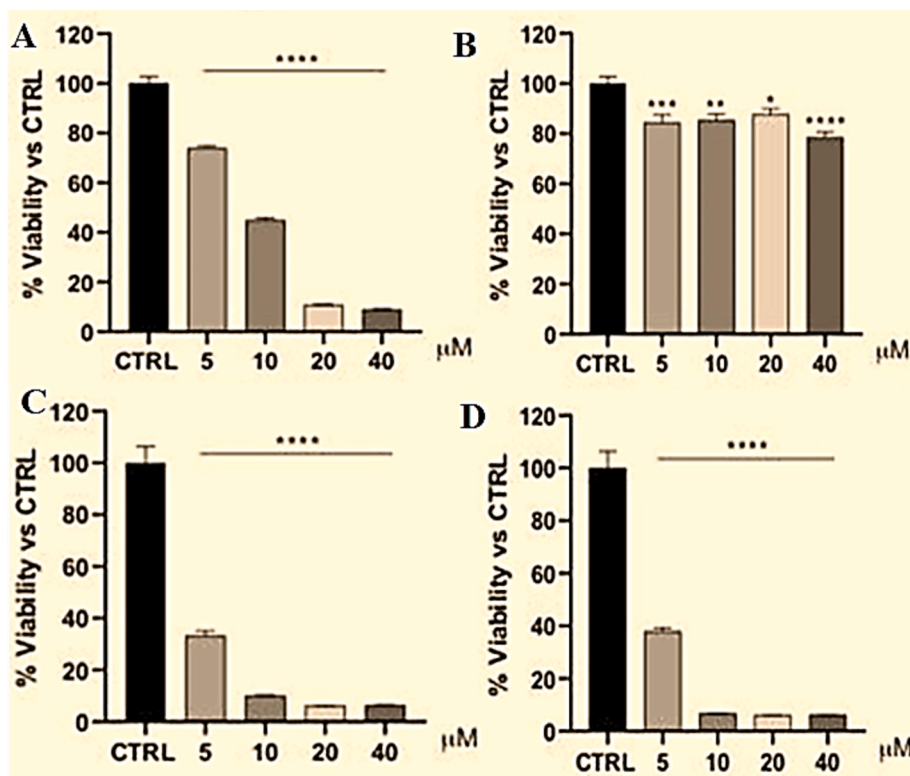


Fig. 13. In vitro cytotoxicity study against MCF-7 at varied concentration for 24 h (incubation period): (A) TM-19 suspension, (B) Blank formulation, (C) TF1, and (D) TM-19 solution (1 % DMSO). (Mean \pm standard deviation, $n = 3$, $p < 0.05$ % for significant variation).

parameters in humans at randomly selected dose of 100 mg in fast subject. Purposely, it was mandatory to investigate the prime pharmacokinetics parameters for the newly synthesized compound to predict valuable information required for formulation development. Moreover, HSPiP programme predicted suitable solvents soluble for TM-19 based on HSP to shorten preliminary formulation development period. Thus, both programs were quite convincing to predict desired goals and objectives for the compound. Based on the experimental and predicted values, topical product could be promising for treating breast cancer and related consequences. Elastic liposomes based topical product was suitable for patients suffering with the cancer. Design Expert optimized the content of composition for maximum drug entrapment, low size, low PDI, and high zeta potential (for stability). Finally, TM-19 suspension, solution, and the optimized TF1 were investigated to compare in vitro cytotoxic potential against breast cell lines MCF-7 for topical delivery. It was clear that TM-19 solution and TF1 exhibited remarkable impact on detrimental effect against MCF-7 as compared to suspension at low dose exposure over period of 24 h. The numerical functional parameter suggested that the low content of PC and high span 80 could be a promising composition to obtain expected elastic liposomes ferrying TM-19. However, the optimized product (suggested with high desirability) still needs to be reformulated for the validation of the right fit of the model by comparison.

CRediT authorship contribution statement

Mohammad A. Altamimi: Funding acquisition, Data curation. **Afzal Hussain:** Writing – original draft, Supervision, Software, Methodology, Investigation, Conceptualization. **Mohammed M. Alanazi:** Methodology, Data curation. **Dhafer Alotaibi:** Methodology, Data curation. **Saeed Ali Syed:** . **Ahmed Bari:** Methodology, Conceptualization.

Funding

The authors extend their appreciation for the research supporting project number (RSPD2024R524), King Saud University, Riyadh, Saudi Arabia.

Declaration of Competing Interest

The authors declare that they have no known competing financial interests or personal relationships that could have appeared to influence the work reported in this paper.

Acknowledgments

The authors are thankful to the Research supporting project number (RSPD2024R524), King Saud University, Riyadh, Saudi Arabia, for this work.

References

- Abbott, S., 2012. An integrated approach to optimizing skin delivery of cosmetic and pharmaceutical actives. *Int. J. Cosmet. Sci.* 34, 217–222.
- Alanazi, M.M., Havranek, T., Bakos, J., Cubeddu, L.X., Castejon, A.M., 2020. Cell proliferation and anti-oxidant effects of oxytocin and oxytocin receptors: role of extracellular signal-regulating kinase in astrocyte-like cells. *Endocr Regul.* 54 (3), 172–182.
- Alhariri, M., Majrashi, M.A., Bahkali, A.H., Almajed, F.S., Azghani, A.O., Khiyami, M.A., Alyamani, E.J., Aljohani, S.M., Halwani, M.A., 2017. Efficacy of neutral and negatively charged liposome-loaded gentamicin on planktonic bacteria and biofilm communities. *Int. J. Nanomedicine.* 12, 6949–6961.
- Aljurbui, S.J., Hussain, A., Yusuf, M., Ramzan, M., Afzal, O., Almohaywi, B., Yasmin, S., Altamimi, A.S.A., 2022. Impact of composition and morphology of ketoconazole-loaded solid lipid nanoparticles on intestinal permeation and GastroPlus-based prediction studies. *ACS Omega.* 7 (26), 22406–22420.
- Alqahtani, S.M., Altharawi, A., Altamimi, M.A., Alossaimi, M.A., Mahdi, W.A., Ramzan, M., Hussain, A., 2022. Method Development, Stability, and Pharmacokinetic Studies of Acyclovir-Loaded Topical Formulation in Spiked Rat Plasma. *Processes.* 10, 2079. <https://doi.org/10.3390/pr10102079>.

- Altamimi, M.A., Hussain, A., Alshehri, S., Imam, S.S., Alnami, A., Bari, A., 2020. A Novel Hemocompatible Imine Compounds as Alternatives for Antimicrobial Therapy in Pharmaceutical Application. *Processes* 8, 1476. <https://doi.org/10.3390/ph8111476>.
- Altamimi, M.A., Hussain, A., Alshehri, S., Imam, S.S., Alnemer, U.A., 2021a. Development and Evaluations of Transdermally Delivered Luteolin Loaded Cationic Nanoemulsion. In *Vitro and Ex Vivo Evaluations*. *Pharmaceutics* 13, 1218.
- Altamimi, M.A., Hussain, A., AlRajhi, M., Alshehri, S., Imam, S.S., Qamar, W., 2021b. Luteolin-Loaded Elastic Liposomes for Transdermal Delivery to Control Breast Cancer. In *Vitro and Ex Vivo Evaluations*. *Pharmaceutics* 14, 1143. <https://doi.org/10.3390/ph14111143>.
- Altamimi, M.A., Hussain, A., Mahdi, W.A., Imam, S.S., Alshammari, M.A., Alshehri, S., Khan, M.R., 2022. Mechanistic insights into luteolin-loaded elastic liposomes for transdermal delivery: HSPiP predictive parameters and instrument-based evidence. *ACS Omega* 7 (51), 48202–48214.
- Bergman, J., Lindstrom, J.O., Tilstam, U., 1988. Synthesis of new indolo[1,2-b]isoquinoline derivatives from N-(2-bromobenzyl)indole. *Tetrahedron* 1988 (41), 2879.
- Bhalani, D.V., Nutan, B., Kumar, A., Singh, C.A.K., 2022. Bioavailability Enhancement Techniques for Poorly Aqueous Soluble Drugs and Therapeutics. *Biomedicines* 10, 2055. <https://doi.org/10.3390/biomedicines10092055>.
- S. Bharanidharan H. Saleem S. Subashchandrabose M. Suresh N.R. Babu FT-IR, FT-Raman and UV-Visible spectral analysis on (E)-N'-(thiophen-2-ylmethylene) nicotinohydrazide *Arch. Chem. Res.* 1 2 2017 1–14. Doi. 10.21767/2572-4657.100007.
- Chauhan, G., Pathak, D.P., Ali, F., Dubey, P., Khasimbi, S., 2022. In-vitro Evaluation of Isatin Derivatives as Potent Anti-Breast Cancer Agents against MCF-7, MDA MB 231, MDA-MB 435 and MDA-MB 468 Breast Cancers Cell Lines: A Review. *Anticancer Agents Med Chem.* 22 (10), 1883–1896.
- Chowdhary, S., Shalini, A.A., Kumar, V., 2022. A Mini Review on Isatin, an Anticancer Scaffold with Potential Activities against Neglected Tropical Diseases (NTDs). *Pharmaceutics* (base). 15 (5), 536. <https://doi.org/10.3390/ph15050536>.
- Comyn, J., 1997. Adhesion Science. Royal society of Chemistry. pp 160, <https://doi.org/10.1039/9781847550064>.
- Corsaro, C., Neri, G., Mezzasalma, A.M., Fazio, E., 2021. Weibull Modeling of Controlled Drug Release from Ag-PMA Nanosystems. *Polymers* 13, 2897. <https://doi.org/10.3390/polym13172897>.
- Gulati, M., Grover, M., Singh, S., Singh, M., 1998. Lipophilic drug derivatives in liposomes. *International Journal of Pharmaceutics* 165 (2), 129–168.
- Guo, H., Diao, Q.-P., 2020. The Anti-Breast Cancer Potential of Bis-Isatin Scaffolds. *Curr Top Med Chem.* 20 (16), 1499–1503.
- C.M. Hansen Hansen solubility parameters: a user's handbook 2nd Edition, 2007 CRC Press page 544 10.1201/9781420006834.
- Hayashi, K., Tatsui, T., Shimanouchi, T., Umakoshi, H., 2013. Membrane interaction between Span 80 vesicle and phospholipid vesicle (liposome): Span 80 vesicle can perturb and hemifuse with liposomal membrane. *Colloids and Surfaces b: Biointerfaces* 106, 258–264.
- Hussain, A., Abdus, S., Mohammad, M., Neyaz, A.M., Zia, U.R., Ahmad, F.J., 2014. Elastic liposome-based gel for topical delivery of 5-fluorouracil: in vitro and in vivo investigation. *Drug Delivery* 1–15. <https://doi.org/10.3109/10717544.2014.976891>.
- Hussain, A., Singh, S., Sharma, D., Webster, T., Shafaat, K., Faruk, A., 2017. Elastic liposomes as novel carriers: recent advances in drug delivery. *International Journal of Nanomedicine* 12, 5087–5108.
- Hussain, A., Altamimi, M.A., Alshehri, S., Imam, S.S., Shakeel, F., Singh, S.K., 2020a. Novel Approach for Transdermal Delivery of Rifampicin to Induce Synergistic Antimycobacterial Effects against Cutaneous and Systemic Tuberculosis Using a Cationic Nanoemulsion Gel. *International Journal of Nanomedicine* 15, 1073–1094.
- Hussain, A., Altamimi, M.A., Alshehri, S., Imam, S.S., Singh, S.K., 2020b. Vesicular elastic liposomes for transdermal delivery of rifampicin: In-vitro, in-vivo and in silico GastroPlus™ prediction studies. *European Journal of Pharmaceutical Sciences* 151, 105411.
- Hussain, A., Afzal, O., Altamimi, M.A., Altamimi, A.S.A., Ramzan, M., Hassan, M.Z., Mahdi, W.A., Webster, T.J., 2022a. Improved subcutaneous delivery of ketoconazole using EpiDerm and HSPiP software-based simulations as assessed by cell viability, cellular uptake, permeation, and hemolysis in vitro Studies. *ACS Omega* 7 (46), 42593–42606.
- Hussain, A., Altamimi, M.A., Imam, S.S., Ahmad, M.S., Alnemer, O.A., 2022b. Green Nanoemulsion Water/Ethanol/Transcutol/LabM-Based Treatment of Pharmaceutical Antibiotic Erythromycin-Contaminated Aqueous Bulk Solution. *ACS Omega* 7 (51), 48100–48112.
- Kesharwani, S.S., Ibrahim, F., 2023. A combined In-Vitro and GastroPlus(R) modeling to Study the Effect of Intestinal Precipitation on Cinnarizine plasma Profile in a fasted state. *AAPS PharmSciTech.* 24 (5), 121. <https://doi.org/10.1208/s12249-023-02577-w>.
- Khan, K.M., Mughala, U.R., Ambreena, N., Khana, A., Perveen, S., Choudhary, M.I., Hee, D.S., Woong, K.J., 2018. Nanoemulsion Vehicles as Carriers for Follicular Delivery of Luteolin. *ACS Biomater. Sci. Eng.* 4 (5), 1723–1729.
- Ma, Z., Hou, L., Jiang, Y., Chen, Y., Song, J., 2014. The endogenous oxindole isatin induces apoptosis of MCF-7 breast cancer cells through a mitochondrial pathway. *Oncol. Rep.* 32 (5), 2111–2117.
- McKerrow, J.H., Chiyanzu, I., Hansell, E., Gut, J., Rosenthal, P.J., Chibale, K., 2003. Synthesis and evaluation of isatins and thiosemicarbazone derivatives against cruzain, falcipain-2 and rhodesain. *Bioorg. Med. Chem. Lett.* 13 (20), 3527.
- Ni, Z., Talattof, A., Fan, J., Tsakalozou, E., Sharan, S., Sun, D., Wen, H., Zhao, L., Zhang, X., 2017. Physiologically based pharmacokinetic and absorption modeling for osmotic pump products. *AAPS J.* 19 (4), 1045–1153.
- Owens, D.K., Wendt, R.C., 1969. Estimation of the surface free energy of polymers. *Journal of Applied Polymer Science.* 13 (8), 1741–1747.
- Saliva, J.F.M., Garden, S.J., Pinto, A., C., 2001. The chemistry of isatins: a review from 1975 to 1999. *J. Braz. Chem. Soc.* 12, 273–324.
- Sharaby, C.M., 2007. Synthesis, spectroscopic, thermal and antimicrobial studies of some novel metal complexes of Schiff base derived from [N1-(4-methoxy-1, 2, 5-thiadiazol-3-yl) sulfanilamide] and 2-thiophene carboxaldehyde. *Spectrochimica Acta Part a: Molecular and Biomolecular Spectroscopy* 66 (4–5), 1271–1278.
- Singh, G., Kalra, P., Singh, A., Sharma, G., Sanchita, P.M., Espinosa-Ruiz, C., Esteban, M. A., 2021. A quick microwave preparation of isatin hydrazone schiff base conjugated organosilicon compounds: Exploration of their antibacterial, antifungal, and antioxidative potentials. *Journal of Organometallic Chemistry.* 953, 122051. <https://doi.org/10.1016/j.jorganchem.2021.122>.
- Smirnov, A.S., Martins, L.M.D.R.S., Nikolaev, D.N., Manzhos, R.A., Gurzhiy, V.V., Krivenko, A.G., Nikolaenko, K.O., Belyakov, A.V., Garabadzhiu, A.V., Davidovich, P. B., 2019. Structure and catalytic properties of novel copper isatin Schiff base complexes. *New Journal of Chemistry* 43 (1), 188–198.
- Snee, R.D., 1971. Design and Analysis of Mixture Experiments. *Journal of Quality Technology.* 3 (4), 159–169.
- Wang, K., Jiang, K., Wei, X., Li, Y., Wang, T., Song, Y., 2021. Physiologically based pharmacokinetic models are effective support for Pediatric Drug Development. *AAPS PharmSciTech.* 22 (6), 208. <https://doi.org/10.1208/s12249-021-02076-w>.
- Wang, D.-Y., van der Mei, H.C., Ren, Y., Busscher, H.J., Shi, L., 2020. Lipid-Based Antimicrobial Delivery-Systems for the Treatment of Bacterial Infections. *Frontiers in Chemistry.* 7. <https://doi.org/10.3389/fchem.2019.00872>.
- Wiśniewski, R., Smieszek, E., Kamińska, E., 1995. Three-dimensional solubility parameters: simple and effective determination of compatibility regions. *Progress in Organic Coatings.* 26 (2–4), 265–274.
- World Health Organization. <https://www.who.int/news-room/fact-sheets/detail/breast-cancer>, accessed on 24th May, 2022.
- Yanar, F., Mosayyebi, A., Nastruzzi, C., Carugo, D., Zhang, X., 2020. Continuous-Flow Production of Liposomes with a Millireactor under Varying Fluidic Conditions. *Pharmaceutics.* 12 (11), 1001.
- Zhao, S., Zhang, X., Tang, M., Liu, X., Deng, J., Zhou, W., Xu, Z., 2023. Design, synthesis and anti-breast cancer properties of butyric ester tethered dihydroartemisinin-isatin hybrids. *Med. Chem. Res.* 32, 705–712.
- Zisman, W.A., 1963. Influence of constitution on adhesion. *Industrial & Engineering Chemistry* 55 (10), 18–38.